2022-06-17

SSVEP-based Brain-computer Interface for Music using a Low-density EEG System

Satvik Venkatesh

Eduardo Reck Miranda *School of Art, Design and Architecture*

Edward Braund

Assistive Technology

The Official Journal of RESNA

ISSN: (Print) (Online) Journal homepage: https://www.tandfonline.com/loi/uaty20

SSVEP-based Brain-computer Interface for Music using a Low-density EEG System

Satvik Venkatesh, Eduardo Reck Miranda & Edward Braund

To cite this article: Satvik Venkatesh, Eduardo Reck Miranda & Edward Braund (2022): SSVEP-based Brain-computer Interface for Music using a Low-density EEG System, Assistive Technology, DOI: 10.1080/10400435.2022.2084182

To link to this article: https://doi.org/10.1080/10400435.2022.2084182

SSVEP-based Brain-computer Interface for Music using a Low-density EEG System

Satvik Venkatesh [a]*, Eduardo Reck Miranda [a], and Edward Braund [a]

[a] *Interdisciplinary Centre for Computer Music Research (ICCMR), University of Plymouth, Plymouth, UK*

*Correspondence: satvik.venkatesh@plymouth.ac.uk

SSVEP-based Brain-computer Interface for Music using a Low-density EEG System

In this paper, we present a bespoke brain-computer interface (BCI), which was developed for a person with severe motor-impairments, who was previously a Violinist, to allow performing and composing music at home. It uses steady-state visually evoked potential (SSVEP) and adopts a dry, low-density, and wireless electroencephalogram (EEG) headset. In this study, we investigated two parameters: (1) placement of the EEG headset and (2) inter-stimulus distance and found that the former significantly improved the information transfer rate (ITR). To analyse EEG, we adopted canonical correlation analysis (CCA) without weight-calibration. The BCI for musical performance realised a high ITR of 37.59 ± 9.86 bits min^{-1} and mean accuracy of 88.89 ± 10.09%. The BCI for musical composition obtained an ITR of 14.91 ± 2.87 bits min^{-1} and a mean accuracy of 95.83 ± 6.97%. The BCI was successfully deployed to the person with severe motor-impairments. She regularly uses it for musical composition at home, demonstrating how BCIs can be translated from laboratories to real-world scenarios.

Keywords: brain-computer interface (BCI); dry electroencephalogram (EEG); computer music; musical composition; musical performance

Word count: 6910 words (5797 words excluding references)

1. Introduction

Brain-computer interfaces (BCIs) for musical applications aim to interface brain waves directly with composition tools, instruments, algorithmic composers, and music players, to name but a few (Eaton et al., 2015; Grierson & Kiefer, 2014; Miranda, 2014). It is beneficial for patients who are suffering from locked-in syndrome, which is the loss of all or most motor abilities, because it provides a means of creative expression, which is shown to have positive effects on mental well-being (Leckey, 2011). It also allows creative practitioners to communicate with musical applications through a novel mechanism of control. Steady-state visually evoked potential (SSVEP) has been widely

adopted by BCIs due to its ease of use and high communication rates (Vialatte et al., 2010; Y. -T. Wang et al., 2011). However, several challenges arise when trying to translate such BCIs from laboratories to real-world scenarios. These include bulky equipment to detect neural activity, poor signal quality among commercial sensors, and environmental factors like light and sound, to name but a few.

Electroencephalogram (EEG) has been popularly used in BCIs because of its non-invasiveness and portability (Nicolas-Alonso & Gomez-Gil, 2012). SSVEP-based BCIs are generally tested with research-grade wet sensors (Bin et al., 2009; Chen et al., 2015b), which provide low impedances in the range of 5 - 10kΩ, that is excellent signal quality for non-invasive detection. However, using wet sensors for real-world scenarios imposes hindrances. Contrarily, dry EEG sensors are more convenient as they are directly placed on the head without additional substances like gel, but suffer from lower signal to noise ratio (SNR). Researchers have explored using dry EEG for SSVEP (Chi et al., 2011; Liu et al., 2019; Mihajlović et al., 2012; Spüler, 2017; Xing et al., 2018). Furthermore, some studies have detected EEG from non-hair bearing areas such as the neck, behind the ears, face, and below the hairline (Carmona et al., 2020; Floriano et al., 2019; Y. -T. Wang et al., 2012, 2017).

In this study, we specifically develop a bespoke SSVEP-based BCI for an individual with severe motor-impairments, who was previously a Violinist, to allow composing music at home. It utilises a dry, wireless, low-density, and portable EEG headset, which detects brain waves through four different electrodes within the 10-20 international system (Jasper, 1958) — Cz, Pz, O1, and O2. Compared to other studies that use dry EEG (Chi et al., 2011; Liu et al., 2019; Mihajlović et al., 2012; Spüler, 2017; Xing et al., 2018), this system uses a smaller number of electrodes, presents a stand-alone system, and applies the BCI for novel musical applications.

The objective of this paper is to develop BCI-based performance and composition tools for a person with a severe motor-impairment condition, such that the system can be used independently in the absence of specialists or engineers. To our knowledge, this is the first study that addresses this task of using BCIs to compose music at home. For this reason, all BCI-related operations are encapsulated into one stand-alone application. In this paper, we adopt joint frequency-phase modulation (JFPM) (Chen et al., 2015b) to present the visual stimulus and canonical correlation analysis (CCA) (Bin et al., 2009; Lin et al., 2007) to analyse EEG.

BCI studies that adopt CCA generally collect training data from users to calibrate weights (Nakanishi et al., 2014). In this study, we adopt CCA without weight-calibration (explained in section 3.4). This does not require user-training sessions and thus, improving the usability of BCIs (Lin et al., 2007; Bin et al., 2009; Nakanishi et al., 2015; Yger et al., 2016). Additionally, this paper investigates 2 parameters — (1) size of and distance between flashing regions in the visual stimulus and (2) placement of the EEG headset. On one hand, Duszyk et al. (2014) demonstrated that there is a linear relationship between the size of the flashing region and SSVEP amplitude. It also stated that inter-stimulus distance does not have a significant effect on SSVEP magnitude. On the other hand, Ng et al. (2012) observed a relationship between inter-stimulus distance and classification accuracy. There were methodological differences between the two studies — one directly measured SSVEP amplitude and the other used a classifier. We understand that the design of visual stimulus has been covered by many studies in the literature. However, these studies were conducted using wet electrodes which have low impedance. Hence, this paper evaluates two different designs for the visual stimulus — one with large flashing squares and the other with smaller flashing squares.

Furthermore, Y. Wang et al. (2006) investigated the effect of electrode location

for SSVEP by using subject-specific electrode placements. Therefore, in this paper, we examine whether the placement of the EEG headset has an effect on the communication rate of the BCI. We are using a commercial and low-cost EEG headset which has a fixed structure with instructions on how to place the headset on the subject's head. However, we investigate if minor adjustments in the placement, which are generally not discussed by headset manufacturers, produce an impact on the communication rate of the BCI. We conduct experiments to investigate this phenomenon.

For practical reasons, we could not visit the individual with motor-impairments to perform extensive tests. Therefore, we conducted experiments with other subjects to investigate parameters before the final deployment.

2. BCI Design

As BCIs are considerably different from conventional musical interfaces (with respect to communication rates and ease of use), design considerations were taken to allow the person with severe motor-impairments to perform and compose music solely by using the BCI. Due to the restricted communication rate, there needs to be a trade-off between flexibility and time taken for composition. We have developed multiple BCI systems with varying degrees of flexibility for composition. For instance, in one system, the user is allowed to choose from several musical pitches, but not control other musical parameters like rhythm. This provides high flexibility to compose melodies. In another system, the user can choose from a fixed set of musical loops that comprise a variation in multiple musical parameters. However, the choice is limited to the loops available at that time.

The operations carried out by the BCI are categorised into 4 sub-operations — providing the visual stimulus, recording EEG signals, analysing the obtained data, and

producing audio/musical output. The specifications of the laptop used in the paper are 17.3 inches, 1920×1080 pixels display, 60 Hz refresh rate, HP ProBook 470 G4 Motherboard i7-7500U, Windows 10, 8 GB RAM, Intel i7 2.7 GHz, NVIDIA graphics GeForce 930MX, and Integrated HD graphics 620.

In this paper, there are 2 types of 6-target BCIs — performance and composition. Under performance, we designed one BCI called *Violin*. Under composition, we designed two BCIs called *Violin composer* and *Violin loops composer*, as shown in figure 1.

For *Violin*, the user can choose from six different musical pitches from the C minor pentatonic scale — C4, D#4, F4, G4, A#4, C5. This BCI allows the user to play a musical instrument. It does not allow the user to compose music, but simply allows them to trigger musical samples and perform with the instrument.

(a) Violin composer

(b) Violin loops composer

Figure 1: Two BCIs for composition.

The next two BCIs enable the user to compose music. The user's compositions would be stored on their computer. *Violin composer* enables the user to create a melody. As shown in figure 1a, the user can make a choice from four different musical pitches, which are randomly displayed by the computer. If the user wishes to choose a note that is not on the screen, the *shuffle* option can be chosen, which would display a fresh set of four musical pitches. After a choice is made by the user, it is added to the composition

stack. Afterwards, the composition up to that instant of time is played back and a new set of musical pitches is displayed. The range of musical pitches is from G3 to G5. We decided to display a random set of pitches instead of an ordered set so that the user need not wait for very long periods for the "ideal" pitch. Instead, the user can either choose a pitch from the displayed options or *shuffle* if none of them are preferable. The *remove* option can be chosen to delete the most recent choice made in the composition. The duration of each note in the composition is constant. A separate *configurations* programme was developed to allow the user to set the duration of each note and the number of notes occurring in the composition.

For *Violin loops composer* (as shown in figure 1a), the user can choose from musical loops. In this context, a musical loop is a short section of pre-recorded sound material that can be directly used in a composition. Hence, the user can use a musical phrase directly instead of individually entering the notes. This approach was adopted to make the interface more interesting for the user and address the low communication rates of BCIs. In this BCI, the user navigates through 18 screens to develop an entire composition. The set of musical choices are unique for each screen. In other words, they depend on the timeline of the composition. This enables the user to build an entire composition from the start. The *play* option allows the user to play the composition until that instant of time and the *remove* option can be used to delete the most recent choice.

3. Materials and Methods

3.1. Visual Stimulus Presentation

This paper adopts JFPM (Chen et al., 2015b) to present the visual stimulus. Each flashing region is encoded with 2 unique attributes — phase and frequency. Generally, in SSVEP, the highest amplitude is elicited for low stimulation frequencies (Chen et al., 2014), which is essential for high-impedance headsets. Hence, our system is a 6-target

BCI with SSVEP frequencies lying in the range of 6.0 Hz to 9.0 Hz equally spaced at 0.6 Hz, as shown in figure 2.

Figure 2: An illustration of the visual stimulus. Frequency and phase values of each region are mentioned (frequency is above and phase is below).

In order to utilise hardware-accelerated rendering and vertical synchronisation (VSync), the visual stimulus is implemented with the help of Open Graphics Library (OpenGL). Vertex shader and fragment shader programmes were written in OpenGL shading language (GLSL). The vertex shader specifies the coordinates of the flashing squares and the fragment shader varies the luminance of the region. The luminance s is varied by equation 1 with the help of sinusoidal stimulation (Manyakov et al., 2013).

$$s = \frac{1}{2}\{1 + \sin(2\pi f t) + \phi\} \quad (1)$$

where f is the stimulation frequency, t is the time, and ϕ is the phase. Rhodes (2010) explains the importance of frame-rate independence during software development. This will be useful for deploying the BCI on multiple platforms that may have varying refresh rates. Hence, in this programme, the value of t is updated every 1 ms. OpenGL textures were used to load graphical icons of musical notation in the BCI as shown in figure 1b.

3.2. Record EEG

EEG signals were recorded from the head with the help of a customised Quick-20 headset manufactured by Cognionics, Inc. The headset comprises 4 electrodes — Cz, Pz, O1, and O2 as shown in figure 3. In addition to the occipital and parietal electrodes,

Cz was added to the set of electrodes because it is commonly chosen as the reference electrode in SSVEP studies (Chen et al., 2015b; Y. -T. Wang et al., 2017). Due to design for manufacturing considerations, we were restricted to choosing electrode positions from the 10-20 international system. Therefore, we were unable to choose electrodes like Oz or POz, which might pick higher amplitudes of SSVEP signals. The sampling rate of the headset is 500 Hz. The headset provides the option to calculate the impedance of electrodes with the help of a carrier wave, which is superimposed with the EEG signals at 125 Hz. Data is transmitted from the headset to the laptop through Bluetooth. A dedicated computer *thread* was written to receive data from the headset.

(a) Electrode positions of the EEG headset.

(b) Components of the EEG headset.

Figure 3: Dry, wireless, and portable EEG headset.

The Cognionics website[1] suggests that for these dry sensors, impedances lie in the range of $100 - 200\ k\Omega$. The following steps were taken to obtain good signal quality. After the headset was applied, the electrodes were adjusted to obtain an impedance of under $1000\ k\Omega$. One useful characteristic of these electrodes is that their contact improves with time (this was verified with the obtained impedance values).

[1] Cognionics: http://www.cognionics.com/wiki/

Subsequently, the electrodes were lightly pressed against the head at regular intervals of time. In all circumstances, for all electrodes, we were able to obtain an impedance of less than $250\ k\Omega$ within 10 minutes. After this, the *carrier wave* was disabled to allow an effective bandwidth of 0 to 125 Hz for the EEG signals.

3.3. Data Analysis

Lin et al. (2007) proposed the idea of using canonical correlation analysis (CCA) for SSVEP to improve communication rates of BCIs. CCA is a multivariate statistical technique that quantifies the relation between 2 sets of variables (Härdle & Simar, 2003). Using this technique, multiple EEG channels can be used for analysis and therefore, it improves the accuracy of BCIs (Bin et al., 2009; Lin et al., 2007). Let X be a matrix comprising samples recorded by the EEG headset as shown in equation 2.

$$X = \begin{pmatrix} Cz[1] & Pz[1] & O1[1] & O2[1] \\ Cz[2] & Pz[2] & O1[2] & O2[2] \\ \vdots & \vdots & \vdots & \vdots \\ Cz[N] & Pz[N] & O1[N] & O2[N] \end{pmatrix} \quad (2)$$

where N is the number of EEG samples considered for analysis. For instance, if the analysis window is 2 s, N is 1000 because the sampling rate of the headset is 500 Hz.

Furthermore, each region in the visual stimulus corresponds to a matrix of reference signals Y, which consists of the fundamental frequency f as shown in equation 3 (Bin et al., 2009).

$$Y = \left(\sin\left[\frac{2\pi fn}{f_s}\right] \quad \cos\left[\frac{2\pi fn}{f_s}\right] \quad \cdots \quad \sin\left[\frac{2\pi(N_h f).n}{f_s}\right] \quad \cos\left[\frac{2\pi(N_h f).n}{f_s}\right]\right) \quad (3)$$

where f is the stimulation frequency, N_h is the number of harmonics, and n is the sample index of the EEG recording. Chen et al. (2015a) showed that 5 was an optimal value for N_h and therefore, in this study, we set N_h to 5.

X and Y are two multi-dimensional variables as defined in equations 2 and 3 respectively. Considering their linear combinations to be $A = XW_X$ and $B = YW_Y$, CCA

finds the weight vectors W_X and W_Y such that the correlation between A and B is maximised. Correlation between A and B is defined by equation 4.

$$\rho(A,B) = \frac{\sum_{n=1}^{N}(a_n-\bar{a})\,(b_n-\bar{b})}{(N-1)s_a s_b} \tag{4}$$

where $A = XW_X$, and $B = YW_Y$, $\rho(A,B)$ is the correlation between A and B, a_n belongs to A, b_n belongs to B, N is the number of samples, $\bar{a}$ is the mean of A, $\bar{b}$ is the mean of B, s_a is the standard deviation of A, and s_b is the standard deviation of B. For a detailed explanation of CCA, refer to studies by Bin et al. (2009); Härdle & Simar (2003); Lin et al. (2007).

3.4. Classification

There are two ways in which CCA can be used for BCIs — with and without weight-calibration. The literature has generally adopted the former technique, where the user trains the system with few trials before actually using it. Weight vectors are calculated over these trials and then averaged. This requires the user to spend additional time training the system (Bin et al., 2009; Chen et al., 2015a, 2015b). In the second technique, which is without weight-calibration, solely the highest correlation value for that specific trial is calculated. The user's choice C is the maximum correlation value calculated among all target frequencies as shown in equation 5 (Bin et al., 2009).

$$C = \max_i \rho_i \tag{5}$$

where ρ is the correlation value for each target i.

The reader is referred to studies by Lin et al. (2007); Bin et al. (2009); Nakanishi et al. (2015); Yger et al. (2016) for more information on CCA without weight-calibration. The advantage of this technique is that it does not require any time to "train" the system. As we were designing the system for a person with severe motor-

impairments, it was not suitable to conduct user-training sessions before using the system. During initial experiments, we tried to conduct user-training sessions with the person. However, the person found it time-consuming and tiring. Furthermore, the training session expects the person to precisely look at specific regions at specified times, which was challenging for the person. Therefore, this paper uses CCA without weight-calibration. CCA calculations were implemented with Eigen[2], which is a C++ template library for linear algebra.

3.5. Relax Time

For *Violin*, the 6 choices presented on the screen were constant. Hence, a relax time of 1 s was given for the user to shift the gaze from one region to another. For *Violin composer* and *Violin loops composer*, the choices presented on the screen were not constant. Thus, the user was given a relax time of 6 s to view and make a musical choice. As this is a prolonged relax time, the user may not expect the squares to start flashing. In order to prevent this, a preparation time of 0.3 s was given after the relax time, during which the icons disappeared and only the borders of the flashing squares were visible. Figure 4 illustrates this process through a flow diagram.

Figure 4: Flow diagram of the BCI composer system.

[2] Eigen: http://eigen.tuxfamily.org/index.php?title=Main_Page

3.6. Audio Output

Each BCI choice had one sound file associated with it. The audio output was played during the relax time. All sound files were stored in Waveform Audio File Format (WAVE or commonly known as WAV). Cross-fading was implemented to have smooth transitions between sound samples. Non-musical choices like *remove*, *play*, and *shuffle* had sound files that uttered the corresponding commands. The composition made by the user was stored as a WAV file in the computer, which can be played by any music player.

3.7. Stimulus Design and EEG Headset Placement

3.7.1. Design of the Visual Stimulus

There were two different stimuli evaluated in this paper, termed as stimulus A and stimulus B. Stimulus A had bigger flashing squares and smaller inter-stimulus distance and stimulus B had smaller flashing squares and bigger inter-stimulus distance. Inter-stimulus distance is defined as the distance between two consecutive flashing squares. Moreover, it is important to note that the size of the flashing squares and inter-stimulus distance are interdependent. If stimulus size is increased, the inter-stimulus distance automatically reduces and vice versa. This is due to the fact that the size of the laptop screen is fixed. The motivations behind exploring different sizes of flashing squares and inter-stimulus distance were: (1) Larger flashing squares might elicit higher magnitudes of SSVEP, (2) larger inter-stimulus distance would have less interference between consecutive flashing squares.

In stimulus A, each flashing region was a square of side 7.62 cm (384 pixels). The horizontal and vertical distances between stimuli were 3.84 cm (192 pixels) and 2.16 cm (108 pixels) respectively. Additionally, the visual angle was calculated by using equation 6 (Baird, 1970; McCready, 1985).

$$V = \tan^{-1}\left(\frac{S}{D}\right) \quad (6)$$

where V is the visual angle, S is the size of the object, and D is the distance between the eye and the object. For our experiments, the user was seated at a distance of approximately 70 cm from the screen and hence, D is equal to 70 cm.

The flashing region subtended a visual angle of 6.25°. The horizontal and vertical gap between stimuli subtended an angle of 3.13° and 1.76° respectively. Ng et al. (2012) stated that an inter-stimulus distance in the range of 5° and 7° improves BCI performance. Therefore, in stimulus B, each flashing region was reduced to a square of side 4.60 cm (230 pixels) and it subtended an angle of 3.75° with the eye. It had equal horizontal and vertical distances of 6.98 cm (350 pixels) and therefore, subtended an angle of 5.70° with the eye.

3.7.2. Placement of EEG Headset

The headset adopted by this paper detects EEG from two electrodes in the occipital region and one electrode in the parietal area. As we are using the same headset for all users (who may have unique head sizes), the electrodes may not reach the required locations on the head. User manuals provided by Cognionics suggested that the ground dry pad sensors are to be placed on the middle region of the forehead. We considered this set-up to be placement A, as shown in figure 5a.

(a) EEG headset deployed according to placement A.

(b) EEG headset deployed according to placement B

(c) Rear view for placement A

(d) Rear view for placement B

Figure 5: Two different headset placements on a subject. The images have been used with the permission of the subject.

In placement B, the ground dry pad sensors were placed as high as possible on the forehead, but making sure that the sensors were not placed on hair (as shown in figure 5b). In other words, it is placed just below the hairline. Effectively, in placement B, the central, parietal, and occipital electrodes move further behind compared to placement A.

Note that the headset has a fixed structure with four electrodes — Cz, Pz, O1, and O2. For placement A and B, we did not adopt any special measures to precisely calculate the position of each electrode with reference to the 10-20 international system, because it was not the goal of the study. However, we aim to find out if minor deviations from the manufacturer's recommendations in placing the EEG headset impacts performance. As we are adopting a dry and high-impedance EEG headset, signals may be sensitive to minor adjustments.

3.7.3. Configurations

In order to evaluate the two parameters mentioned above, there were 4 different configurations of the BCI — C1: placement A and stimulus A, C2: placement A and stimulus B, C3: placement B and stimulus A, and C4: placement B and stimulus B.

(a) Electrode positions for placement A

(b) Electrode positions for placement B

Figure 5: Rear view of a subject wearing the headset for both placements.

3.8. Offline Experiment

As mentioned earlier, we were unable to visit the individual with severe motor-impairments to perform extensive tests. This was due to the following reasons. Our laboratory and the individual were located in different cities. Furthermore, most of our time with the person was dedicated to understanding her expectations from the composer system, explaining the BCI system to her, and enabling her carer to set-up the system for her independently, without our supervision. Therefore, our BCI system was optimised and tested separately on 6 subjects.

All experimental procedures were approved by the University's ethics committee. 6 healthy subjects (5 males and 1 female) in the age range of 23 to 55 years participated in the experiments. All subjects were experienced with the process of musical composition and had a normal or corrected-to-normal vision. The experiment was conducted in a dark room. Subjects were asked to minimise body movements and keep electronic gadgets away. During the experiment, subjects were requested to avoid eye blinks. However, there were no methods adopted to detect unintentional eye movements.

The laptop screen was placed approximately 70 cm away from the user. Initially, one of the four configurations was randomly chosen and the system was set-up accordingly. Six targets were present on the screen. A green colour visual cue indicated which target the subject was supposed to look at, which was randomly chosen by the

computer. The cue appeared for 0.7 s and the users were asked to immediately shift their gaze to the corresponding region. Subsequently, for the preparation time, only borders of the 6 regions were visible for 0.3 s.

After 1 s ($0.7\ s + 0.3\ s$), all regions flashed at their respective frequencies for 4 s. Each test case consisted of six appearances (or six trials) of visual cues (that is, one for each target) in random order. After two test cases, subjects were asked to close their eyes and rest for few minutes. For each configuration, four test cases were acquired from each user. The same procedure was followed for all four configurations and hence, a total of sixteen test cases was obtained from all users.

3.9. Data Processing

In EEG recordings, we observed high magnitude under 1 Hz and a peak at 50 Hz. High-pass and notch filters at 4 Hz and 50 Hz respectively were applied on EEG data. Both were Butterworth filters and zero-phase filtering was performed. The filter was designed in MATLAB and code generator was used to translate the code to C++ for the JUCE application. In visual-based BCIs, a visual latency of 7 to 15 ms is generally observed (Russo & Spinelli, 1999). Therefore, this study discarded the first 20 ms of EEG data after the onset of the stimulus.

3.10. SNR

In order to compare the four configurations, SNR values were calculated. For each EEG channel, fast Fourier transform (FFT) was performed to obtain the amplitude spectrum $y(f)$ for a data length of 4 s, where f stands for frequency. For a SSVEP frequency , SNR was defined as the ratio of the amplitude spectrum at f and the average of K neighbouring frequencies, as shown in equation 7 (Y. Wang et al., 2006; Y. -T. Wang et al., 2017).

$$SNR = \frac{K \times y(f)}{\sum_{k=1}^{K}[y(f+k\Delta f)+y(f-k\Delta f)]} \quad (7)$$

where Δf is the frequency resolution (0.6 Hz in this paper) and K is equal to 6. Among the 4 EEG channels, the maximum SNR value was taken for comparison. The SNR values were averaged over all SSVEP frequencies.

3.11. Performance Evaluation

In order to evaluate the performance of the BCI, classification accuracy and ITR were calculated. Accuracy is defined as the ratio of the number of correct predictions and the total number of trials. For example, if the green colour visual cue highlights the fourth target, the user's brain waves are analysed through CCA and a prediction is made. If the fourth region is predicted by the analysis, then it is a correct prediction. Otherwise, it is a wrong prediction. For each trial, only the order in which the targets occur was randomised. Therefore, within each trial, all the six targets are highlighted exactly once. For each configuration, the total number of trials was 24 (4 $test\ cases\ \times 6\ targets$).

ITR has been defined by equation 8 (Chen et al., 2014; Wolpaw et al., 2002).

$$ITR = \frac{60}{T}\left[\log_2 N + plog_2 p + (1-p)\log_2\left(\frac{1-p}{N-1}\right)\right] \quad (8)$$

where T is the trial time in seconds, N is the number of flashing regions, and p is the mean accuracy averaged over all targets. The relax time for *Violin* is 1 s. For *Violin composer* and *Violin loops composer*, the relax time and preparation adds up to 6.3 s. These durations were added to the trial time while calculating ITR.

4. Results

4.1. SNR

Two-way repeated measures ANOVA was performed to compare the configurations. The two factors for analysis were the parameters — placement and stimulus. The significance level was set at 0.05. SNR values of C3 and C4 (placement B) were higher

than C1 and C2 (placement A). The mean SNRs for the configurations were $C1 = 3.33 \pm 1.17$, $C2 = 3.60 \pm 1.18$, $C3 = 4.04 \pm 1.49$, and $C4 = 4.05 \pm 1.53$. Placement had a significant effect on SNR ($p = 0.001$) and stimulus did not have a significant effect on SNR ($p = 0.179$). Figure 6 shows the SNR for different configurations.

Figure 6: The maximal SNR across all stimulation frequencies for different configurations.

4.2. Classification Accuracy

For all four configurations, one-way repeated measures ANOVA showed that there were significant differences in accuracy for different data lengths ($p < 0.001$). Figure 7 shows the classification accuracy of the four configurations for different data lengths. C3 and C4 (placement B) performed better than C1 and C2 (placement A) for all four data lengths — 1 s, 2 s, 3 s, and 4 s. Two-way repeated measures ANOVA was performed for these data lengths. The two factors were placement and stimulus. The significance level was set at 0.05.

Figure 7: Classification accuracy for different data lengths. Note that the accuracies for all the BCI systems are equal, but their ITRs can vary because of different relax times.

The accuracy values for all four data lengths is given in table 1. For data lengths — 2 s, 3 s, and 4 s, the placement of the EEG headset had a significant effect on performance ($p < 0.05$). Furthermore, there was no significant interaction between the factors ($p > 0.05$). Hence, placement B considerably improves the performance of the BCI.

Table 1: Accuracy of different configurations and data lengths. † indicates that there was a statistically significant difference for placement and * indicates that there was a statistically significant difference for the stimulus size.

4.3. ITR

4.3.1. Violin

C1, C3, and C4 obtained their highest ITRs for a data length of 2 s, which are $C1 = 32.02 \pm 12.43$ bits min^{-1}, $C3 = 36.64 \pm 14.07$ bits min^{-1}, and $C4 = 37.59 \pm 9.86$ bits min^{-1}. C2 obtained its highest ITR for a data length of 3 s, which was 26.20 ± 12.46 bits min^{-1}. Figure 8a shows the ITR of *Violin* for different configurations.

(a) ITR for different data lengths in *Violin*.

(b) ITR for different data lengths in *Violin composer* and *Violin loops composer*.

Figure 8: ITRs of both BCIs for different configurations.

4.3.2. Composer

C1 and C2 obtained their highest ITRs for a data length of 4 s, which was $\mathrm{C1} = 12.69 \pm 2.98$ bits min^{-1} and $\mathrm{C2} = 12.12 \pm 2.17$ bits min^{-1}. C3 and C4 obtained their highest ITRs for a data length of 3 s, which was $\mathrm{C3} = 15.03 \pm 2.13$ bits min^{-1} and $\mathrm{C4} = 14.91 \pm 2.87$ bits min^{-1}. Figure 8 shows the ITRs of the BCIs for different configurations.

4.3.3. Optimal Configuration

In this paper, C3 and C4 consistently obtained higher ITRs than C1 and C2. Considering other factors such as increasing the number of flashing regions in future research and smaller stimuli causing less visual fatigue, C4 was chosen as the optimal configuration. Table 2 shows the accuracy and ITR values of individual subjects for both types of BCIs using C4.

Table 2: Accuracy and ITR values of all subjects for *Violin* (data length is 2 s) and the composer BCIs (data length is 3 s) that adopt C4: placement B and stimulus B.

4.4. Online Experiment

Violin was tested by asking the user to choose all options successively in a clockwise manner, starting from the first option. For *Violin composer*, subjects were asked to choose the duration of note and length of melody by using the *configurations* programme. After doing so, they composed a melody. While composing, if the BCI detected a wrong choice or the user did not like the choice after listening to it, the *remove* option was used. For *Violin loops composer*, subjects composed an entire song by using the BCI. All songs and melodies composed by using the BCIs were sent to the users after the experiment.

There were no measures taken to calculate accuracy or ITR for the online experiment because of the complex control flow of the BCI. This was due to the following reasons. Generally, accuracy and ITR in BCI spellers are calculated by asking the user to type a specific sentence. However, we asked the users to compose music using the BCI and this cannot be fixed beforehand. Additionally, the *remove* option in a BCI speller is used if a word was typed incorrectly. However, in our system, the user used the *remove* option also if they did not like the sound of it, after listening to the composed melody. Due to the above reasons, we were not able to calculate the accuracy and ITR during the online experiments.

As you can see in table 3, the composer BCI had a high mean accuracy of 95.43% for an analysis window of 3 s. Therefore, the feedback from most users was that the BCI generally selected the correct option. We also tested all the BCI systems — *Violin*, *Violin composer*, and *Violin loops composer* on the person with motor impairments. She successfully used all the musical systems. First, the carer deployed the EEG headset on the person with motor impairments. Subsequently, she was asked which of the three musical systems she would like to play. Although the person with motor impairmnets could not provide an answer through speech, there were subtle

means of communication such as nodding and smiling which the carer could understand. Later, the configurations program was set by the carer, which specified the duration of note and length of melody. Then, the person with motor impairments played and composed music with the BCI system.

As mentioned earlier, most of our time with the person was dedicated to understanding her expectations from the composer system, explaining the BCI system to her, and enabling her carer to set-up the system for her independently, without our supervision. Therefore, we were unable to calculate the ITR of her using the system due to time and funding constraints. However, her feedback was that the system listened to the choices made by her.

5. Concluding Discussions

In this paper, we presented a portable high-speed BCI that used a dry, low-density, and wireless EEG headset. It was applied to three musical systems — *Violin*, *Violin composer*, and *Violin loops composer*. It was a bespoke system developed for a person with severe motor-impairments to allow composing music at home. It adopted JFPM (Chen et al., 2015b) and CCA (Bin et al., 2009; Lin et al., 2007) for visual stimulation and EEG data analysis respectively. For relax times of 1 s and 6.3 s, the system obtained an ITR of 37.59 ± 9.86 bits min^{-1} and 14.91 ± 2.87 bits min^{-1} respectively. The mean accuracies were $88.89 \pm 10.09\%$ and $95.83 \pm 6.97\%$ respectively. The ITR obtained in this paper surpasses the performances in studies that use dry electrodes (Chi et al., 2011; Mihajlović et al., 2012; Y. -T. Wang et al., 2017). The improvement in performance is attributed to an optimal placement of the EEG headset. However, Xing et al. (2018) obtained a higher ITR than this paper but used a greater number of electrodes. Our BCI's performance can be improved by increasing the number of electrodes and the electrode density in the occipital and parieto-occipital region.

Furthermore, multiple studies have shown that calibration or user-training improves the performance of BCI systems (Nakanishi et al., 2014; Wong et al., 2020). As we developed a bespoke BCI-based musical system for one user, it would be beneficial to have some user-training sessions in future research. This way, communication rate of the BCI could be boosted.

This paper found that headset placement significantly improved the performance of the BCI. This encourages researchers to explore different headset placements and find an optimal one for their task. If they are adopting dry EEG, minor adjustments in placement may significantly alter communication rates. The guidelines provided by the manufacturer need not be optimal for the placement of the EEG headset. Moreover, in this study inter-stimulus distance did not have a significant effect, however, we analysed only two different designs for the visual stimulus. The difference in their performances was not significant, however, a variety of designs need to be tested to confirm the relationship between inter-stimulus distance and performance of the BCI. The optimal configuration for the BCI was C4: placement B and stimulus B. The BCI was successfully delivered to the person with motor-impairments. Video and text-based user manuals were created to enable the carer to set-up the BCI. We witnessed the carer set-up the BCI and the person use all the three musical systems to compose music. The *configurations* programme was set-up by the carer communicating with the individual. Figure 9 is a picture of the person using the BCI. We have been in touch with the person, and she regularly composes music using the BCI.

Figure 9: A picture of the individual using the BCI to compose music.

Future research would explore alternative headset designs with more electrodes in the occipital and parieto-occipital region. For instance, an electrode combination of POz, Oz, O1, and O2 might be more suitable for SSVEP. As this paper adopted a dry and wireless EEG headset, other consumer grade systems (Hairston et al., 2014) such as the Emotive EPOC, Advanced Brain Monitoring's B-Alert X10, and g.NAUTILUS RESEARCH by g.tec, to name but a few, can be adopted for our BCI-based musical systems. In this paper, we ensured that the impedance of the electrodes was under $250\ k\Omega$. Therefore, if a reader wishes to reproduce this work on another commercial-grade EEG headset, the impedance needs to be below $250\ k\Omega$ to ensure reasonable signal quality. Furthermore, researchers have proposed alternative stimulation paradigms like steady-state motion visual evoked potential (SSMVEP) (Yan et al., 2017), which might be more convenient due to the absence of flashing stimuli and be more interesting for musical systems.

Disclosure statement

The authors report no conflict of interest.

Funding

This study was partially funded by the School of Humanities and Performing Arts, University of Plymouth and GREY Advertising, London.

References

Baird, J. C. (1970). *Psychophysical Analysis of Visual Space: Int. Series of Monographs in Experimental Psychology* (Vol. 9). Elsevier.

Bin, G., Gao, X., Yan, Z., Hong, B., & Gao, S. (2009). An Online Multi-channel SSVEP-based Brain-computer Interface using a Canonical Correlation Analysis Method. *J. Neural Eng., 6*, 046002.

Carmona, L., Diez, P. F., Laciar, E., & Mut, V. (2020). Multisensory stimulation and EEG recording below the hair-line: a new paradigm on brain computer interfaces. *IEEE Transactions on Neural Systems and Rehabilitation Engineering*.

Chen, X., Chen, Z., Gao, S., & Gao, X. (2014). A High-ITR SSVEP-based BCI Speller. *Brain-Computer Interfaces, 1*, 181–191.

Chen, X., Wang, Y., Gao, S., Jung, T.-P., & Gao, X. (2015a). Filter Bank Canonical Correlation Analysis for Implementing a High-speed SSVEP-based Brain–computer Interface. *J. Neural Eng., 12*, 046008.

Chen, X., Wang, Y., Nakanishi, M., Gao, X., Jung, T.-P., & Gao, S. (2015b). High-speed Spelling with a Noninvasive brain-computer Interface. *Proc. Nat. Acad. Sci., 112*, E6058–E6067.

Chi, Y. M., Wang, Y.-T., Wang, Y., Maier, C., Jung, T.-P., & Cauwenberghs, G. (2011). Dry and noncontact EEG sensors for mobile brain–computer interfaces. *IEEE Trans. Neural Syst. Rehabil. Eng., 20*, 228–235.

Duszyk, A., Bierzyńska, M., Radzikowska, Z., Milanowski, P., Kuś, R., Suffczyński, P., . . . Durka, P. (2014). Towards an Optimization of Stimulus Parameters for Brain-computer Interfaces based on Steady State Visual Evoked Potentials. *PLoS One, 9*, e112099.

Eaton, J., Williams, D., & Miranda, E. (2015). The space between us: evaluating a multi-user affective brain-computer music interface. *Brain-Computer Interfaces, 2*, 103–116.

Floriano, A., Carmona, V. L., Diez, P. F., & Bastos-Filho, T. F. (2019). A study of SSVEP from below-the-hairline areas in low-, medium-, and high-frequency ranges. *Research on Biomedical Engineering, 35*, 71–76.

Fransson, F. (1966). The Source Spectrum of Double-reed Wood-wind Instruments. *Royal Institute of Technology, Stockholm, Speech Transmission Lab, QPSR, 4*, 35.

Grierson, M., & Kiefer, C. (2014). Contemporary approaches to music BCI using P300 event related potentials. In *Guide to Brain-Computer Music Interfacing* (pp. 43–59). Springer.

Härdle, W., & Simar, L. (2003). *Applied Multivariate Statistical Analysis.* Springer.

Hairston, W. D., Whitaker, K. W., Ries, A. J., Vettel, J. M., Bradford, J. C., Kerick, S. E., & McDowell, K. (2014). Usability of four commercially-oriented EEG systems. Journal of neural engineering, 11(4), 046018.

Jasper, H. H. (1958). The ten-twenty electrode system of the Int. Federation. *Electroencephalogry Clinical Neurophysiology, 10*, 370-375.

Leckey, J. (2011). The therapeutic effectiveness of creative activities on mental well-being: a systematic review of the literature. *J. psychiatric and mental health nursing, 18*, 501–509.

Levine, S. P., Huggins, J. E., BeMent, S. L., Kushwaha, R. K., Schuh, L. A., Passaro, E. A., . . . Ross, D. A. (1999). Identification of electrocorticogram patterns as the basis for a direct brain interface. *Journal of clinical neurophysiology, 16*(5).

Lin, Z., Zhang, C., Wu, W., & Gao, X. (2007, 6). Frequency recognition based on canonical correlation analysis for SSVEP-based BCIs. *IEEE Trans. Biomed. Eng., 54*, 1172-1176. doi:10.1109/TBME.2006.889197

Liu, Z., Wang, Y., Pei, W., Xing, X., Gui, Q., & Chen, H. (2019). A High-Resolution Dry Electrode Array for SSVEP-Based Brain-Computer Interfaces. *2019 9th International IEEE/EMBS Conference on Neural Engineering (NER)*, (pp. 811–814).

Manyakov, N. V., Chumerin, N., Robben, A., Combaz, A., van Vliet, M., & Van Hulle, M. M. (2013). Sampled Sinusoidal Stimulation Profile and Multichannel Fuzzy Logic Classification for Monitor-based Phase-coded SSVEP Brain-computer Interfacing. *J. Neural Eng., 10*, 036011.

McCready, D. (1985). On size, distance, and visual angle perception. *Perception & Psychophysics, 37*, 323–334.

Mellinger, J., Schalk, G., Braun, C., Preissl, H., Rosenstiel, W., Birbaumer, N., & Kübler, A. (2007). An MEG-based brain–computer interface (BCI). *Neuroimage*, *36*(3), 581–593.

Mihajlović, V., Garcia-Molina, G., & Peuscher, J. (2012). Dry and water-based EEG electrodes in SSVEP-based BCI applications. *Int. Joint Conf. Biomed. Eng. Syst. Tech.*, (pp. 23–40).

Miranda, E. R. (2014). Brain-Computer Music Interfacing: Interdisciplinary Research at the Crossroads of Music, Science and Biomedical engineering. In E. R. Miranda, & J. Castet (Eds.), *Guide to Brain-computer Music Interfacing* (pp. 1–27). Springer.

Nakanishi, M., Wang, Y., Wang, Y.-T., Mitsukura, Y., & Jung, T.-P. (2014). A high-speed brain speller using steady-state visual evoked potentials. *Int. J. Neural syst., 24*, 1450019.

Nakanishi, M., Wang, Y., Wang, Y. T., & Jung, T. P. (2015). A comparison study of canonical correlation analysis based methods for detecting steady-state visual evoked potentials. *PloS one, 10(10)*, e0140703.

Ng, K. B., Bradley, A. P., & Cunnington, R. (2012). Stimulus specificity of a steady-state visual-evoked potential-based brain–computer interface. *J. Neural Eng., 9*, 036008.

Nicolas-Alonso, L. F., & Gomez-Gil, J. (2012). Brain computer interfaces, a review. *Sensors, 12*, 1211–1279.

Rhodes, G. (2010). Real-Time Game Physics. In S. Rabin (Ed.), *Introduction to Game Development* (Second ed., pp. 387-419). Charles River Media.

Russo, F. D., & Spinelli, D. (1999). Electrophysiological evidence for an early attentional mechanism in visual processing in humans. *Vision research, 39*, 2975–2985.

Spüler, M. (2017). A high-speed brain-computer interface (BCI) using dry EEG electrodes. *PloS one, 12*.

Vialatte, F.-B., Maurice, M., Dauwels, J., & Cichocki, A. (2010). Steady-state Visually Evoked Potentials: Focus on Essential Paradigms and Future Perspectives. *Prog. Neurobiol., 90*, 418-438.

Wang, Y., Chen, X., Gao, X., & Gao, S. (2017). A Benchmark Dataset for SSVEP-Based Brain–Computer Interfaces. *IEEE Trans. Neural Syst. Rehabil. Eng., 25*, 1746–1752.

Wang, Y., Wang, R., Gao, X., Hong, B., & Gao, S. (2006). A Practical VEP-based Brain-computer Interface. *IEEE Trans. Neural Syst. Rehabil. Eng.*, *14*, 234–240.

Wang, Y.-T., Nakanishi, M., Wang, Y., Wei, C.-S., Cheng, C.-K., & Jung, T.-P. (2017). An online brain-computer interface based on SSVEPs measured from non-hair-bearing areas. *IEEE Trans. Neural Syst. Rehabil. Eng.*, *25*, 14–21.

Wang, Y.-T., Wang, Y., & Jung, T.-P. (2011). A cell-phone-based brain–computer interface for communication in daily life. *J. Neural Eng.*, *8*, 025018.

Wang, Y.-T., Wang, Y., Cheng, C.-K., & Jung, T.-P. (2012). Measuring steady-state visual evoked potentials from non-hair-bearing areas. *Eng. in Medicine and Biology Society (EMBC), 2012 Annual Int. Conference of the IEEE*, (pp. 1806–1809).

Wang, Y.-T., Wang, Y., Cheng, C.-K., & Jung, T.-P. (2013). Developing Stimulus Presentation on Mobile Devices for a Truly Portable SSVEP-based BCI. *Eng. in Med. Biol. Soc.*, (pp. 5271–5274).

Wolpaw, J. R., Birbaumer, N., McFarland, D. J., Pfurtscheller, G., & Vaughan, T. M. (2002). Brain–computer interfaces for communication and control. *Clinical neurophysiology*, *113*, 767–791.

Wong, C. M., Wang, B., Wang, Z., Lao, K. F., Rosa, A., & Wan, F. (2020). Spatial filtering in SSVEP-based BCIs: Unified framework and new improvements. IEEE Transactions on Biomedical Engineering, 67(11), 3057-3072.

Xing, X., Wang, Y., Pei, W., Guo, X., Liu, Z., Wang, F., . . . Chen, H. (2018). A high-speed SSVEP-based BCI using dry EEG electrodes. *Scientific reports*, *8*, 14708.

Yan, W., Xu, G., Li, M., Xie, J., Han, C., Zhang, S., . . . Chen, C. (2017). Steady-state motion visual evoked potential (SSMVEP) based on equal luminance colored enhancement. *PloS one*, *12*, e0169642.

Yger, F., Berar, M., & Lotte, F. (2016). Riemannian approaches in brain-computer interfaces: a review. *IEEE Transactions on Neural Systems and Rehabilitation Engineering*, *25*(10), 1753-1762.

List of Tables

Table 1: Accuracy of different configurations and data lengths. † indicates that there was a statistically significant difference for placement and * indicates that there was a statistically significant difference for the stimulus size.

Data Length	**Accuracy (%)**			
	C1	**C2**	**C3**	**C4**
$1\ s$	42.36 ± 11.61	41.66 ± 17.87	54.16 ± 21.41	49.31 ± 10.34
$2\ s^{\dagger *}$	82.63 ± 14.30	70.13 ± 24.78	86.81 ± 14.77	88.89 ± 10.09
$3\ s^{\dagger}$	87.49 ± 13.44	83.33 ± 22.97	96.52 ± 4.87	95.83 ± 6.97
$4\ s^{\dagger}$	93.74 ± 9.41	88.89 ± 23.22	96.52 ± 6.67	98.61 ± 2.15

Table 2: Accuracy and ITR values of all subjects for *Violin* (data length is 2 s) and the composer BCIs (data length is 3 s) that adopt C4: placement B and stimulus B.

Subject	**Accuracy (%)**		**ITR ($bits\ min^{-1}$)**	
	2 s	**3 s**	**2 s**	**3 s**
S1	95.83	100.00	44.76	16.67
S2	91.67	91.67	39.56	12.76
S3	95.83	100.00	44.76	16.67
S4	95.83	100.00	44.76	16.67
S5	70.83	83.34	20.73	9.98
S6	83.34	100.00	30.96	16.67
Mean	**88.89 ± 10.09**	**95.83 ± 6.97**	**37.59 ± 9.86**	**14.91 ± 2.87**

List of Figures

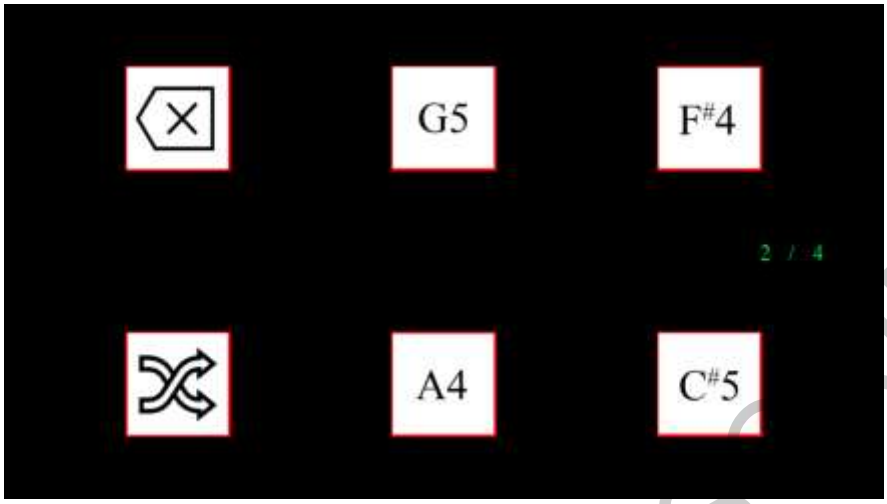

(a) Violin composer

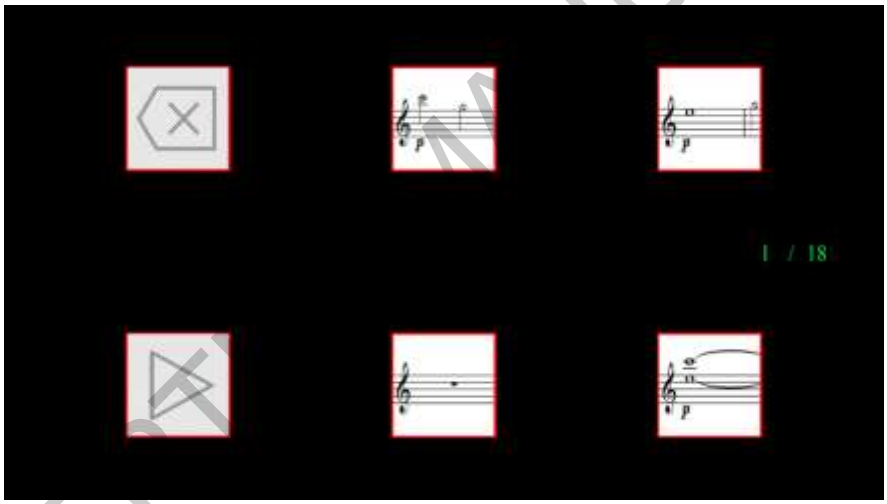

(b) Violin loops composer

Figure 1: Two BCIs for composition.

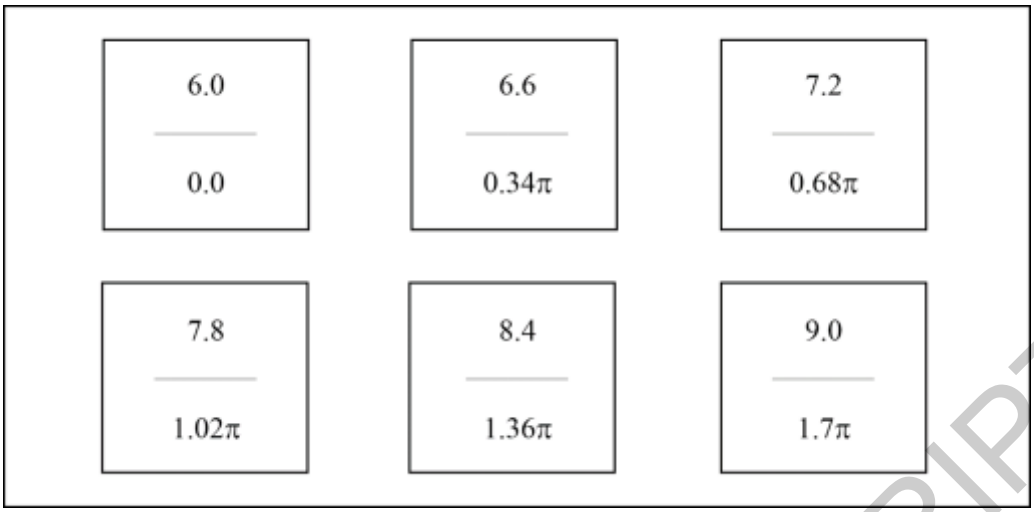

Figure 2: An illustration of the visual stimulus. Frequency and phase values of each region are mentioned (frequency is above and phase is below).

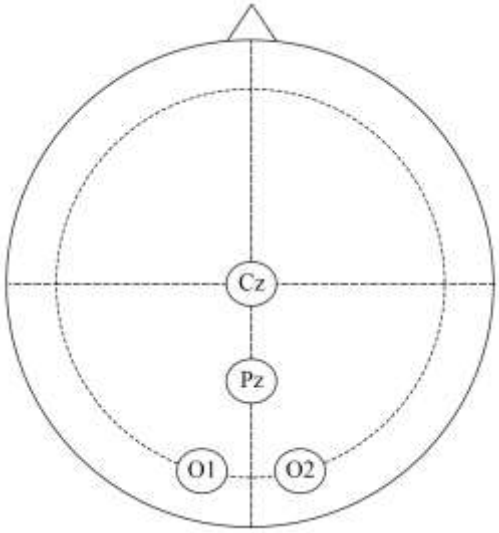

(a) Electrode positions of the EEG headset

(b) Components of the EEG headset.

Figure 3: Dry, wireless, and portable EEG headset.

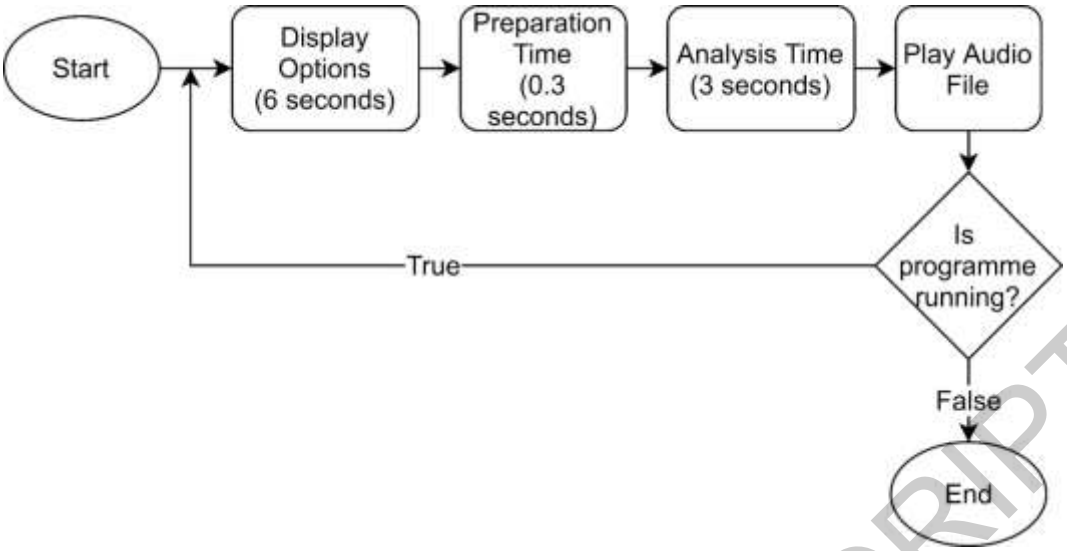

Figure 4: Flow diagram of the BCI composer system.

(a) EEG headset deployed according to placement A.

(b) EEG headset deployed according to placement B.

(c) Rear view for placement A.

(d) Rear view for placement B.

Figure 5: Two different headset placements on a subject. The images have been used with the permission of the subjects.

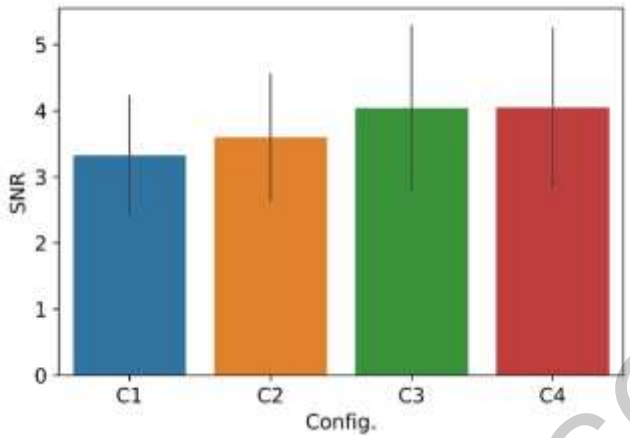

Figure 6: The maximal SNR across all stimulation frequencies for different configurations. Error bars indicate the standard deviation.

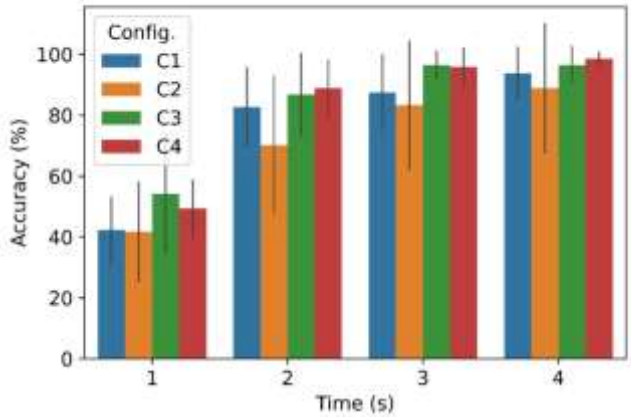

Figure 7: Average classification accuracy for different data lengths. The error bars indicate the standard deviation. Note that the accuracies for all the BCI systems are equal, but their ITRs can vary because of different relax times.

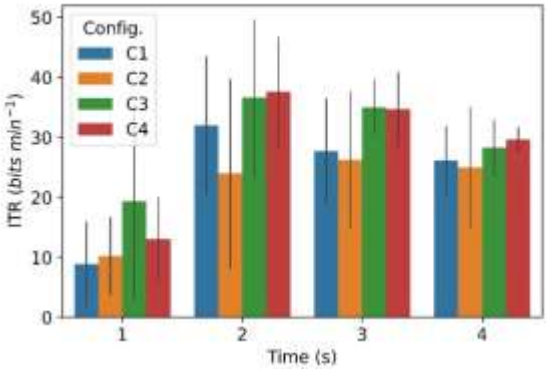

(a) ITR for different data lengths in *Violin*.

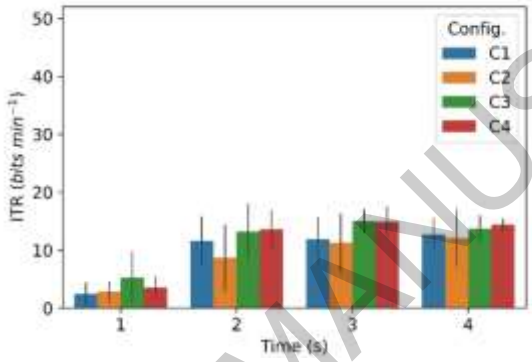

(b) ITR for different data lengths in *Violin composer* and *Violin loops composer*.

Figure 8: ITRs of both BCIs for different configurations.

Figure 9: A picture of the individual using the BCI to compose music.

Figure captions

Figure 1 (a): Violin composer

Figure 1 (b) Violin loops composer

Figure 1: Two BCIs for composition.

Figure 2: An illustration of the visual stimulus. Frequency and phase values of each region are mentioned (frequency is above and phase is below).

Figure 3 (a) Electrode positions of the EEG headset

Figure 3 (b) Components of the EEG headset.

Figure 3: Dry, wireless, and portable EEG headset.

Figure 4: Flow diagram of the BCI composer system.

Figure 5 (a) EEG headset deployed according to placement A.

Figure 5 (b) EEG headset deployed according to placement B

Figure 5 (c) Rear view for placement A

Figure 5 (d) Rear view for placement B

Figure 5: Two different headset placements on a subject. The images have been used with the permission of the subject.

Figure 6: The maximal SNR across all stimulation frequencies for different configurations. The error bars indicate the standard deviation.

Figure 7: Average classification accuracy for different data lengths. The error bars indicate the standard deviation. Note that the accuracies for all the BCI systems are equal, but their ITRs can vary because of different relax times.

Figure 8 (a) ITR for different data lengths in *Violin*.

Figure 8 (b) ITR for different data lengths in *Violin composer* and *Violin loops composer*.

Figure 8: ITRs of both BCIs for different configurations.

Figure 9: A picture of the individual using the BCI to compose music.

List of Alternative Text for figures

Figure 1(a): A screenshot of the Violin composer interface. It has six buttons for the user to choose from, among which four are musical notes, one is to delete, and one is to shuffle.

Figure 1(b): A screenshot of the Violin loops composer interface. It has six buttons for the user to choose from, among which four are musical loops, one is to delete, and one is to play.

Figure 2: Six square buttons present on the screen. Within each button, the corresponding frequency and phase is written.

Figure 3(b): An illustration of the electrode positions based on the 10-20 International system.

Figure 3(b): A picture of the EEG headset. The different components of the headset are labelled.

Figure 4: Flow diagram of the BCI composer system

Figure 5(a): A person wearing the EEG headset.

Figure 5(b): A person wearing the EEG headset.

Figure 5(c): Rear view of a person wearing the EEG headset.

Figure 5(d): Rear view of a person wearing the EEG headset.

Figure 6: A bar chart showing the SNR for each configuration. The SNR of C3 and C4 are considerably higher than C1 and C2.

Figure 7: A line chart with time on the x-axis and accuracy on the y-axis. The accuracies of C3 and C4 are the highest. C1 is lower and C2 is much lower.

Figure 8(a): A line chart with time on the x-axis and ITR on the y-axis. The ITRs of C3 and C4 are the highest. C1 is lower and C2 is much lower.

Figure 8(b): A line chart with time on the x-axis and ITR on the y-axis. The ITRs of C3 and C4 are the highest. C1 is lower and C2 is much lower.

Figure 9: A person wearing an EEG headset and is looking at a computer.